Strategies to Stabilize New Members of the $(A_3A'BO_6)_\alpha(A_3B_3O_9)_\beta$ Homologous series in the Sr-Rh-O System: Structure of the One-Dimensional ($\alpha = 3, \beta = 2$) $[Sr_{10}(Sr_{0.5}Rh_{1.5})_{TP}(Rh_6)_{Oh}]O_{24}$ Oxide

Khalid Boulahya,[a] María Hernando,[a] Aurea Varela,[a] José M. González-Calbet,*[a] Marina Parras,[a] and Ulises Amador[b]

Abstract: The ($\alpha = 3$, $\beta = 2$) member of the $(A_3A'BO_6)_\alpha(A_3B_3O_9)_\beta$ homologous series has been stabilised in the Sr-Rh-O system for a $[Sr_{10}(Sr_{0.5}Rh_{1.5})_{TP}(Rh_6)_{Oh}]O_{24}$ composition. The structural characterisation has been performed by powder X-ray and electron diffraction measurements and high-resolution electron microscopy. In this structure, three face-sharing $[RhO_6]$ octahedra linked by one $[Rh/SrO_6]$ trigonal prism comprise the infinite one-dimensional chain that runs parallel to the c axis of a trigonal unit cell ($P\bar{3}c1$), with parameters $a = 9.6411(1)$ and $c = 21.2440(4)$ Å.

Keywords: electron diffraction · rhodium · scanning probe microscopy · strontium

Introduction

A large number of one-dimensional oxides adopt structures formed by the ordered intergrowth between the 2H-$BaNiO_3$[1] and the K_4CdCl_6[2] structural types. The former, with the general formula 2H-ABO_3, is built up of isolated chains of $[BO_6]$ face-sharing octahedra running along the c axis and separated by columns of A atoms. The latter, also formulated as $A_3(A'B)O_6$, shows similar features but the chains are now formed by alternating octahedral (O_h) and trigonal prismatic (TP) units linked by common faces in a stacking sequence 1:1. Intermediate phases reported in several systems[3–6] can be defined by the general formula $(A_3A'BO_6)_\alpha(A_3B_3O_9)_\beta$ in which B stands for cations in O_h coordination and A′ refers to cations in TP environment.

When A′ = B both polyhedra sites are occupied by the same metal; in this case the metal adopts different oxidation states. This is the case of the A-Co-O system (A = Ca, Sr, Ba) for which a lot of oxides have been reported between the limiting phases $Ca_3Co_2O_6$ and 2H-$BaCoO_3$.[7–9] A similar situation has been described in the A-Rh-O system (A = Sr, Ba) when the materials are synthesised as single crystals. Up to now, two phases have been reported: $Ba_9Rh_8O_{24}$,[10] isostructural to $Ba_9Co_8O_{24}$,[7] and $Sr_6Rh_5O_{15}$,[11] isostructural to $Sr_6Co_5O_{15}$,[12] which here after will be referred as [9:8] and [6:5] phases, respectively. $Ba_9Rh_8O_{24}$ oxide ($\alpha = 3$, $\beta = 6$) is formed by the ordered intergrowth, along the c axis, of seven octahedra and one trigonal prism sharing faces; in $Sr_6Rh_5O_{15}$ ($\alpha = 3$, $\beta = 3$), strings of four octahedra are linked by one face-sharing trigonal prism along the same direction.

A different situation, regarding the polyhedra occupation, appears in the A-Rh-O system when samples are prepared in polycrystalline form. Actually, when A = Ba, a few rhodium vacancies are necessary in order to stabilise the [9:8] structure, ($\alpha = 3$ $\beta = 6$), leading to the composition $Ba_9Rh_{7.92}O_{24}$.[13] On the other hand, for A = Sr, the ($\alpha = 3$, $\beta = 3$) member of the series, is stabilised for a Rh/Sr = 0.7 cationic ratio, lower than that corresponding of the $Sr_6Rh_5O_{15}$ (Rh/Sr = 0.83). This deviation from the ideal stiochiometry has been attributed to the presence of Rh vacancies in the structure.[14] The structural characterisation of this powdered phase, carried out by means of electron diffraction measurements and high-resolution electron microscopy, shows a fivefold superstructure of the [6:5] subcell along the c axis.

Up to now, only one other one-dimensional Sr/Rh oxide has been fully characterised in this system. Actually, the ($\alpha = 3$, $\beta = 0$) end-member of this $(A_3A'BO_6)_\alpha(A_3B_3O_9)_\beta$ homologous series is described by the composition Sr_4RhO_6. Rh atoms are located at the centre of the octahedral site, whereas the Sr atoms occupy the trigonal-prismatic sites, according to the $Sr_3[(Sr)_{TP}(Rh)_{Oh}]O_6$ cationic distribution (i.e., A′ = A).[15]

As stated above, the Sr-Rh-O compounds show some particular features, such as the presence of metal vacancies

[a] Prof. J. M. González-Calbet, Dr. K. Boulahya, M. Hernando, Dr. A. Varela, Dr. M. Parras
Dpto. Química Inorgánica
Facultad de Ciencias Químicas
Universidad Complutense de Madrid, 28040-Madrid (Spain)
Fax: (+34) 91-3944342
E-mail: jgcalbet@quim.ucm.es

[b] Dr. U. Amador
Dpto. Química Inorgánica y Materiales
Facultad de Ciencias Experimentales y Técnicas
Universidad San Pablo, Urb. Montepríncipe
Boadilla del Monte, 28668 Madrid (Spain)

  0947-6539/02/0821-4973 $ 20.00+.50/0

and a partial substitution of Rh atoms by alkaline-earth ions into the polyhedra chains; this situation is not observed in other A-M-O (M = Co; Ni) systems that form one-dimensional oxides.[7–9, 16] This makes it very difficult to design a synthesis procedure for the intermediate phases. In this sense, the structure corresponding to the ($\alpha=3$, $\beta=2$) member, ($A_5B_4O_{12}$, when A′ = B), is built up of isolated rows of three O_h and one TP unit sharing faces along the c axis; the A cations occupy empty sites in between the chains.[8] Considering that the unit cell contains two of this $3O_h$-1TP sequences, a more correct formulation for this phase is $A_{10}B_8O_{24}$. Taking into account the particularities found in the phases in the Sr-Rh-O system described above, it is not easy to establish the most adequate Sr/Rh cationic ratio to obtain the member with $\alpha=3$ and $\beta=2$. In fact, depending on the polyhedra occupation, different possibilities arise. If the TP sites are fully occupied by Sr atoms, as in Sr_4RhO_6, the composition should be $Sr_{10}[(Sr_2)_{TP}(Rh_6)_{Oh}]O_{24}$. In contrast, if all the TP and O_h sites are fully occupied by Rh atoms, the composition should be $Sr_{10}[(Rh_2)_{TP}(Rh_6)_{Oh}]O_{24}$. Finally, if Rh vacancies are present in the structure, as found in $Ba_9Rh_{7.92}O_{24}$, the corresponding stoichiometry could be formulated as $Sr_{10}Rh_{8-x}O_{24}$ $(0<x\leq 1)$. Moreover, intermediate situations cannot be discarded.

In an attempt to shed light on this complex system, this work is devoted to the search for the thermodynamic conditions to stabilise the ($\alpha=3$, $\beta=2$) member of the $(A_3A'BO_6)_\alpha(A_3B_3O_9)_\beta$ homologous series. For this purpose, assuming as starting points the two simplest compositions $Sr_{10}(Sr_2Rh_6)O_{24}$ (Sr/Rh = 12/6) and $Sr_{10}Rh_8O_{24}$ (Sr/Rh = 10/8), we have explored different Sr/Rh stoichiometries. We report in this paper the detailed synthesis conditions and the structural characterisation, by means of X-ray diffraction (XRD), selected area electron diffraction (SAED) and high-resolution electron microscopy (HREM), of the ($\alpha=3, \beta=2$) member of the Sr/Rh oxide series, that is, the [5:4] structure.

Results

The Sr/Rh = 12:6 nominal cationic ratio: As mentioned above, the Sr/Rh = 12:6 ratio corresponds to the $Sr_{10}[(Sr_2)_{TP}(Rh_6)_{Oh}]O_{24}$ stoichiometry associated with the ($\alpha=3$, $\beta=2$) structure when the TP sites are occupied by Sr^{2+} ions. It is evident that this (Sr/Rh) cationic ratio also corresponds to the well-known [2:1] layered phase, that is, Sr_2RhO_4.[17] This phase, which constitutes the $n=1$ term of the Ruddlesden and Popper series,[18] is stabilised as a single phase from 1150 °C to 1200 °C. Therefore, in order to explore whether the [5:4] structure is obtained, the synthesis has been tried in the temperature range between 1050 and 1150 °C. At lower temperatures, starting materials are still detected in the XRD patterns. All attempts to synthesise the $Sr_{10}[(Sr_2)_{TP}(Rh_6)_{Oh}]O_{24}$ phase were unsuccessful; a phase mixture was always obtained in which the layered Sr_2RhO_4 was, by far, the majority phase.

The Sr/Rh = 10:8 nominal cationic ratio: The Sr/Rh = 10:8 cationic ratio corresponds to the $Sr_{10}[(Rh_2)_{TP}(Rh_6)_{Oh}]O_{24}$ stoichiometry, in which all the oxygen polyhedra in the [5:4] structure are occupied by Rh atoms. The XRD pattern corresponding to a sample with this nominal cationic ratio, treated at 1060 °C in air, is shown in Figure 1a. The whole

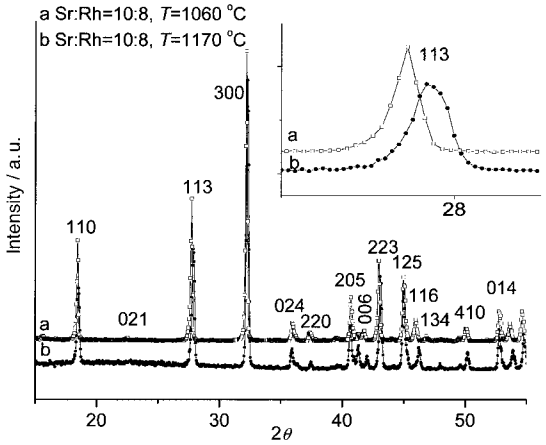

Figure 1. XRD patterns corresponding to the 10/8 Sr/Rh nominal cationic ratio sample heated in air at a) 1060 °C and b) 1170 °C. Inset: detail of the XRD patterns around the $(113)_{6:5}$ maximum.

pattern can be indexed on the basis of a rhombohedral unit cell of parameters $a=9.6$, $c=65$ Å and corresponds to the ($\alpha=3$, $\beta=3$) member of the series;[14] no extra reflections were detected. No structural change is observed by XRD pattern in the temperature range between 1060 and 1150 °C.

In order to confirm this result, a study by means of selected area electron diffraction (SAED) and energy dispersive spectroscopy (EDS) was carried out. As we have previously reported, from the SAED characterization, the $[1\bar{2}10]$ reciprocal plane provides the more useful structural information. Actually, this reciprocal plane enables us to obtain directly the values of α and β, that is, the number of the different structural blocks constituting the structure, and, thus, to identify the different members of the $(A_3A'BO_6)_\alpha$-$(A_3B_3O_9)_\beta$ homologous series. For this purpose, the SAED pattern must be described as a modulated superstructure of the hexagonal 2H subcell. The superstructure direction corresponds to $[\alpha+\beta\,\alpha+\beta\,i2\alpha]^*_{2H}$. In this case, the SAED pattern along the $[1\bar{2}10]$ zone axis is shown in Figure 2. All the checked crystals are identical and show the same SAED pattern. The most intense spots correspond to hexagonal 2H planes (referred as subindex 2H in Figure 2). The modulation direction, marked with an arrow, follows the reciprocal $[66i6]_{2H}$ direction, confirming that the ($\alpha=3$, $\beta=3$) term, that is, the [6:5] structure, is stabilised. However, besides the most intense spots (corresponding to the ideal [6:5] structure) a set of very weak maxima, along the $[0001]_{6:5}$ direction, are visible. Such maxima correspond to a fivefold superstructure of the basic [6:5] subcell. These microstructural features are those corresponding to the ($\alpha=3$, $\beta=3$) Sr/Rh oxide.[14]

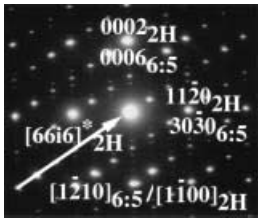

Figure 2. SAED pattern corresponding to the [6:5] phase along $[1\bar{2}10]$.

0947-6539/02/0821-4974 $ 20.00+.50/0 Chem. Eur. J. 2002, 8, No. 21

Besides, as previously reported, such a member is stabilized for a cationic ratio Sr/Rh = 10:7.5 as also found from the EDS analysis (Figure 3). Therefore, both SAED and EDS results

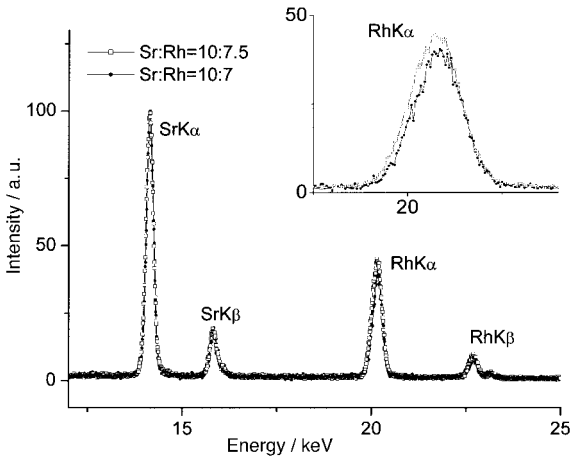

Figure 3. EDS spectra corresponding to the crystals showing the SAED of Figure 2 (□) and the SAED of Figure 4 (●). The Rh Kα line is shown in the inset.

indicate that, for a Sr/Rh = 10:8 nominal cationic ratio, the ($\alpha = 3$, $\beta = 3$) term is the only stable one-dimensional phase formed in the temperature range between 1060 and 1150 °C. Interestingly enough, a structural evolution is observed when the temperature is increased above 1150 °C. Figure 1b shows the XRD pattern corresponding to the sample when heated at 1170 °C for three days. Although the general features remains unchanged, when comparing both X-ray patterns (Figure 1a and b) slight but meaningful differences can be appreciated. First at all, a slight broadening of the diffraction maxima corresponding to the (*hkl*) reflections with $l \neq 0$ can be observed. Besides, such maxima are displaced to higher 2θ values. SAED and EDS characterisation give more evidence on the origin of this evolution. In fact, after this thermal treatment, a phase mixture is obtained. Among the different type of crystals found in this batch, a small fraction give the SAED pattern depicted in Figure 4. The features of this pattern along the $[1\bar{2}10]$ zone axis are those corresponding to the [5:4] phase. Actually, although basic spots characteristic of the 2H type are kept, note that the modulation now follows the $[55i6]_{2H}$ reciprocal direction (marked with an arrow in the figure) of the 2H subcell, as previously reported for $Sr_5Co_4O_{12}$, which crystallises in the *P*3*c*1 space group.[9] The diffraction conditions observed in the reciprocal plane shown in Figure 4, (*00l*) $l = 2n$, are also in agreement with the *P*3*c*1 space group. These results prove the existence of the [5:4] phase ($\alpha = 3$, $\beta = 2$) in the Sr-Rh-O system.

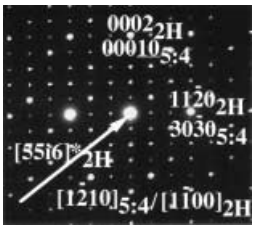

Figure 4. SAED pattern corresponding to the [5:4] phase along $[1\bar{2}10]$ zone axis found in the Sr/Rh = 10:8 nominal cationic ratio when heated at 1170 °C.

In order to determine the actual Sr/Rh cationic ratio stabilising that structure, EDS analyses were performed on these crystals. As it can be appreciated from Figure 3, the obtained Sr/Rh cationic ratio is very close to that corresponding to the previous phase (also depicted in Figure 3) although a slightly smaller Rh content is observed. In fact, the EDS analysis of these crystals gives a cationic Sr/Rh ratio ranging from 10:7.2 to 10:6.8 leading to an average Sr/Rh = 10/7 cationic ratio.

The Sr/Rh = 10:7 cationic ratio: On the basis of the above results, we have prepared a polycrystalline sample with the Sr/Rh = 10:7 composition as described in the Experimental Section. The corresponding XRD pattern is depicted in Figure 5. The whole pattern can be indexed with a trigonal [5:4] unit cell of parameters $a = 9.6$ and $c = 21.2$ Å.

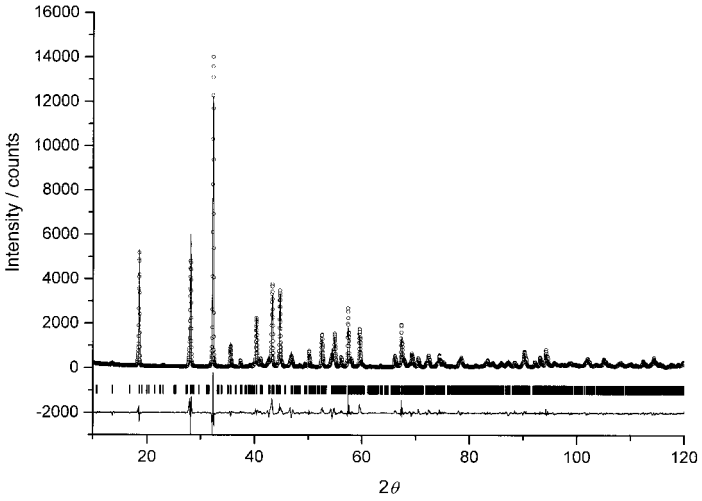

Figure 5. Graphic results of the fitting of the X-ray powder diffraction data of $Sr_{10.5}Rh_{7.5}O_{24}$: experimental (points), calculated (solid line) and difference (bottom).

The microstructural study of this sample was carried out by means of SAED and HREM measurements. Besides the $[1\bar{2}10]$ reciprocal plane, already observed in Figure 4, the relevant SAED patterns correspond to the [0001] and $[1\bar{1}00]$ zone axes are shown in Figure 6a and b, respectively. In the [0001] reciprocal plane, reflections are distributed in a hexagonal array corresponding to a lattice parameter close to 9.8 Å, in agreement to the XRD results. All the (*hk*0) reflections are visible in agreement with the trigonal *P*3*c*1 space group proposed for the [5:4] structure. In addition, the SAED pattern along the $[1\bar{1}00]$ zone axis is also in agreement with the trigonal unit cell of this phase although (00*l*), $l \neq 2n$, reflections appear as a result of dynamic diffraction effects. Therefore, the essential features of all SAED patterns are those characteristic of the [5:4] structure. Neither extra ordering nor streaking is detected.

The HREM taken along the $[1\bar{2}10]$ zone axis (Figure 6c) shows the structural features of the [5:4] phase. Actually, the *d* spacings close to 10 and 8.3 Å correspond to d_{002} and d_{100}, respectively. Moreover, the observed contrast is also the characteristic of this structure: the alternance of two bright dots and three less bright dots along the [0001] direction has been associated with the ordered intergrowth of 1TP and $3O_h$

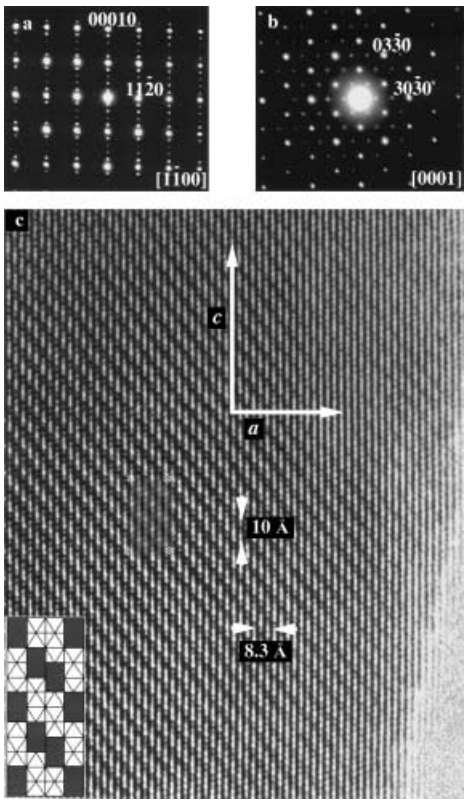

Figure 6. SAED patterns corresponding to the [5:4] phase along a) [0001] and b) [1$\bar{1}$00] zone axes. c) HREM along the [1$\bar{2}$10] direction. Projected model along this direction is included. Simulated image ($\Delta t = 4$ and $\Delta f = -90$ nm) is shown at the inset.

polyhedra, according to the [...3Oh-1TP-3Oh-1TP...] sequence that comprises the [5:4] polyhedra chains which run parallel to the *c* axis. A schematic representation of this structure model is included in Figure 6c. From the ideal atomic coordinates of the [5:4] structure, we performed an image calculation. This simulated image (inset at Figure 6c) fits nicely with the experimental one for $\Delta t = 4$ and $\Delta f = -90$ nm.

At this stage of the study, it can be stated that the ($\alpha = 3$, $\beta = 2$) term has been stabilized as single phase for a Sr/Rh = 10/7 cationic ratio. However, it is difficult to establish the corresponding stoichiometry, since with this cationic ratio at least two different formulas can be proposed for this term. Actually, if rhodium vacancies are present in the structure, $Sr_{10}Rh_7\square_1O_{24}$, should be the correct stoichiometry. In contrast, if all the oxygen polyhedra are fully occupied, both Rh as well as Sr cations must be incorporated in the polyhedra chains in order to preserve the above cationic ratio. In this case, the resulting stoichiometry should be close to $Sr_{10.5}(Sr_{0.5}Rh_{7.5})O_{24}$.

The structure refinement from powder XRD data can be helpful in order to detect the presence, or not, of cationic vacancies in this phase. Since SAED and HREM data suggest that the obtained compound is isostructural to $Sr_5Co_4O_{12}$,[9] the structure of this stoichiometric oxide was used as starting model for the refinement of the XRD data. However, along the refinement process it was clear than there was no reason for the structure to be acentric. Thus, a structural model was developed in the centrosimetric $P\bar{3}c1$ space group (no. 165) instead of the $P3c1$ (no. 158) proposed for the cobalt-containing oxide. Figure 5 shows the graphic result of the fitting of the experimental X-ray diffraction pattern for the Sr/Rh ($\alpha = 3$, $\beta = 2$) oxide and the difference between the observed and the calculated data. The final structural parameters are collected in Table 1, whereas Table 2 gives some selected interatomic distances. A schematic representation of the structure is depicted in Figure 7.

Table 1. Final structural parameters corresponding to $Sr_{10.5}Rh_{7.5}O_{24}$.[a]

Atom	*x*/*a*	*y*/*b*	*z*/*c*	Occupancy
Sr(1)	0.686(1)	0.019(1)	0.0488(3)	1
Sr(2)	0.337(1)	0.019(1)	0.1585(2)	1
Sr(3)	0.656(2)	0	1/4	1/2
Rh(1)	0	0	0	1/6
Rh(2)	2/3	1/3	0.1681(6)	1/3
Rh(3)	1/3	2/3	0.2916(6)	1/3
Rh(4)	0	0	0.1185(6)	1/3
Rh(5)	0	0	1/4	1/6
Rh(6)	1/3	2/3	0.0404(6)	1/3
Rh(7)	1/3	2/3	0.4146(6)	1/3
O(1)	0.172(6)	−0.015(6)	0.064(2)	1
O(2)	0.151(5)	0.609(5)	0.108(2)	1
O(3)	0.506(7)	0.178(7)	0.030(2)	1
O(4)	0.332(7)	0.846(7)	0.234(2)	1
O(5)	0.144(6)	0.195(5)	0.182(2)	1
O(6)	0.496(5)	0.352(6)	0.156(2)	1

[a] Space group $P\bar{3}c1$ (no. 165), $a = 9.6403(2)$, $c = 21.2396(4)$ Å, $V = 1709.50(5)$ Å^3, $B_{overall}(A^2) = 0.10(4)$ $R_B = 0.097$, $R_{exp} = 0.064$, $R_{wp} = 0.16$, $\chi^2 = 7.8$.

Table 2. Selected interatomic distances (up to 3.10 Å) in $Sr_{10.5}Rh_{7.5}O_{24}$.

Sr(1)−O(1) ×2	2.76(6)	Rh(1)−O(1) ×6	2.20(5)
Sr(1)−O(1)′	2.69(5)		
Sr(1)−O(2)	2.34(5)	Rh(2)−O(2) ×3	2.02(5)
Sr(1)−O(3)	2.86(7)	Rh(2)−O(4) ×3	2.22(6)
Sr(1)−O(3)′	2.62(6)		
Sr(1)−O(3)″	2.51(5)	Rh(3)−O(4) ×3	2.12(6)
Sr(1)−O(6)	2.69(5)	Rh(3)−O(6) ×3	2.07(5)
Sr(2)−O(1)	2.48(5)	Rh(4)−O(1) ×3	2.09(5)
Sr(2)−O(2)	2.68(5)	Rh(4)−O(5) ×3	2.16(6)
Sr(2)−O(4)	2.30(6)		
Sr(2)−O(4)′	2.67(6)	^{TP}Rh(5)−O(5) ×6	2.22(5)
Sr(2)−O(5)	3.10(6)		
Sr(2)−O(5)′	2.45(6)	^{TP}Rh(6)−O(2) ×3	2.11(5)
Sr(2)−O(6)	2.78(5)	^{TP}Rh(6)−O(3) ×3	2.13(6)
Sr(2)−O(6)′	2.61(6)		
		Rh(7)-O(3) ×3	1.93(6)
Sr(3)−O(4) ×2	2.73(8)	Rh(7)−O(6) ×3	2.30(5)
Sr(3)−O(4)′ ×2	2.80(6)		
Sr(3)−O(5) ×2	2.26(6)	Rh(1) − Rh(4)	2.52(1)
Sr(3)−O(5)′ ×2	2.45(5)	Rh(4) − ^{TP}Rh(5)	2.79(1)
Rh(2) − Rh(3)	2.62(1)		
		Rh(3) − Rh(7)	2.61(1)
		Rh(7) − ^{TP}Rh(6)	2.67(1)
		^{TP}Rh(6)− Rh(2)	2.71(2)

It is worth pointing out, that the structure refinement of this type of one-dimensional oxide presents some serious problems, such as a strong preferred orientation effect due to the pronounced hexagonal shape of the crystallites. Another important point to be considered is the relatively weak scattering factor of oxygen atoms when compared to heavy

0947-6539/02/0821-4976 $ 20.00+.50/0 *Chem. Eur. J.* **2002**, *8*, No. 21

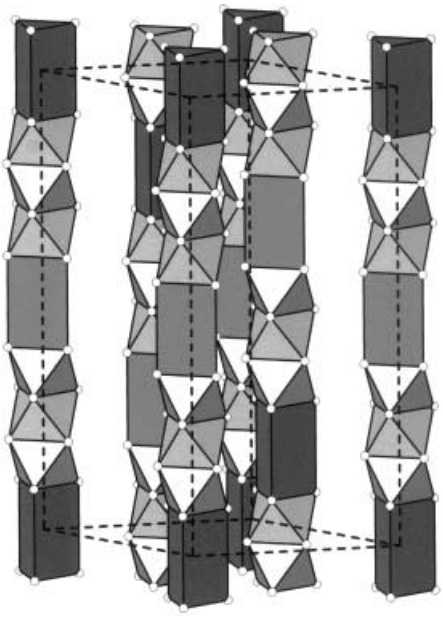

Figure 7. Schematic representation of the $Sr_{10.5}Rh_{7.5}O_{24}$ structure.

atoms such as Sr and Rh. In spite of this, the refinement was stable and it was possible to refine the positions of the oxygen atoms, provided an overall temperature factor is used. Thus, the metal-to-oxygen distances in Table 2 should be considered with some care though the metallic coordination, that is, the polyhedron defined by the closest oxygen atoms around a given metal, is undoubtedly correct. According to this, the Sr atoms are eight-coordinate through oxygen at distances ranging from 2.25 to 3.10 Å, in very distorted polyhedra. On the other hand, Rh(5) and Rh(6) occupy positions in the trigonal prism, whereas the other Rh atoms are octahedrally coordinated by nearby oxygen atoms at the distances given in Table 2. The obtained values for all M–O distances are reasonable and consistent with previously reported bond lengths in comparable Sr/Rh oxides.[11, 15]

Inside the chains, the Rh–Rh inter-octahedral distances (in Table 2 the Rh atoms in trigonal prisms are labelled with "TP") are very close to those found in 4H or 18H-$BaRhO_3$ (2.5–2.6 Å).[19] However, of the two Rh–Rh distances between Rh atoms in a trigonal prism and Rh atoms in neighbouring octahedra, one is significantly longer (about 2.80 Å) than the other (2.60 Å). This structural feature has also been observed in the one-dimensional oxide $Ba_9Rh_{7.92(2)}O_{24}$.[13] The enlargement of the distance between TP–O_h metals compared to that shown by Oh–Oh metals seems to be inherent in these one-dimensional oxides, since it is also observed in others similar oxides, such as $Ba_6Ni_5O_{15}$[16] and $Sr_6Co_5O_{15}$.[11]

On the other hand, in our [5:4] Sr/Rh oxide no short Rh–Rh distance is observed. In a previous paper[13] the existence of a significantly shorter Rh-–Rh distance was associated to some metal deficiency (4%) in one of the involved Rh positions. Thus, this suggests that the degree of vacancies in this compound should be very low, if any. Since this is a very important point with regard to the crystal chemistry of this kind of compound, we have refined the occupancies of all the rhodium sites. In all cases, the refined occupancy was higher than the maximum allowed by the site multiplicity, and so the occupancy was fixed at this value (Table 1). We have also checked the Sr positions, which in all cases must be considered as fully occupied. Concerning the oxygen sublattice, no conclusive evidence can be obtained from powder XRD data, but we can assume that the anionic sublattice is also complete, since in this kind of compound there is no evidence of oxygen vacancies. Thus, the material should be considered as a stochiometric compound, in the sense that both, the metal and the oxygen positions are completely filled.

On the basis of these results, the presence of Rh vacancies, at least in the high concentration corresponding to a $Sr_{10}Rh_7\square_1O_{24}$ stoichiometry, can be discarded. Therefore, the presence of Sr, besides Rh, into the polyhedra chains can be established. Moreover, taking into account the size of Sr^{2+} ions relative to the Rh ions, it is reasonable to think that Sr^{2+} is incorporated into the trigonal prismatic sites, leading to a situation similar to that found in $Sr_3Sr_{TP}Rh_{Oh}O_6$, the ($\alpha=3$, $\beta=0$) member in which Sr occupies all the TP sites. In the ($\alpha=3$, $\beta=2$) member, only a fraction of these sites, close to one of every four, seems to be occupied by Sr giving the $[Sr_{10}(Sr_{0.5}Rh_{1.5})_{TP}(Rh_6)_{Oh}]O_{24}$ stoichiometry, which agrees with the Sr/Rh = 10:7 cationic ratio. Unfortunately, the X-ray scattering factors of Rh and Sr ions are similar (they differ by six electrons) and, in fact, they are indistinguishable by using powder XRD techniques. To corroborate this cationic composition a different and independent method must be used. In this context it is worth noting that assuming the usual valences for Sr and O, the average Rh atom oxidation state is +3.6, indicating the presence of both Rh^{IV} and Rh^{III} in the polyhedra chains. Spectroscopic techniques could give some information on the actual Rh oxidation state and, therefore, about the actual chemical composition. The latter could be also obtained by thermal analysis. Both kinds of data are discussed in the following.

On the basis of the above ideas, a XPS study of the $[Sr_{10}(Sr_{0.5}Rh_{1.5})_{TP}(Rh_6)_{Oh}]O_{24}$ sample was carried out. Two different Sr/Rh mixed oxides, in which the Rh oxidation state is well established, were used as standard compounds. For that purpose, $SrRh_2O_4$[20] and Sr_2RhO_4[17] were chosen. Unfortunately, all the spectra seem to be essentially the same and no conclusive results can be obtained. This is most likely because the surface of all the samples, even when freshly prepared, is hydrated. In fact, the most intense contribution to the spectra is attributed to the surface species, whilst the relevant information contained in the less intense contributions is hidden by the background. Attempts to eliminate the surface contamination by different in situ thermal treatments in vacuum were unsuccessful because of a partial decomposition of the sample.

To obtain complementary information about the actual composition of the sample, thermogravimetric analysis under a reducing atmosphere was performed. A representative TGA curve is shown in Figure 8; SrO and Rh metal are the residual products as determined by XRD. If the anionic sublattice is complete, that is, 24 atoms per unit formula, the cationic composition can be deduced from the weight loss. However, it is worth stressing that the above-mentioned

  0947-6539/02/0821-4977 $ 20.00+.50/0

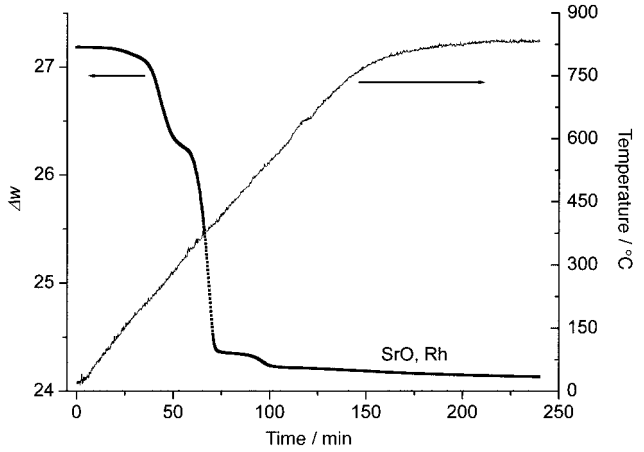

Figure 8. TGA curve corresponding to $Sr_{10.5}Rh_{7.5}O_{24}$ sample.

superficial hydration of the sample is also reflected in this TGA curve. The starting point of the TGA trace is not well defined leading to an uncertainty in the data obtained in this case that is larger than normal. From these data, the calculated cationic composition is in the range Sr/Rh = 10.5 (2):7.5(2) per unit formula. Although this result should be regarded with some care, it agrees with the EDS analyses and supports the XRD results concerning the actual composition. Thus, the ($\alpha = 3$, $\beta = 2$) member of this one-dimensional homologous series in the Sr-Rh-O system must be formulated as $[Sr_{10}(Sr_{0.5}Rh_{1.5})_{TP}(Rh_6)_{Oh}]O_{24}$.

Conclusion

From the ensemble of the information provided by the experimental data, we can conclude that the ($\alpha = 3$, $\beta = 2$) member of the $(A_3A'BO_6)_\alpha(A_3B_3O_9)_\beta$ homologous series is also stable in the Sr-Rh-O system. The corresponding TP-$(Oh)_3$-TP polyhedra sequence is stabilised through the incorporation of some Sr^{2+} cations, besides Rh ions, into the polyhedra chains. This yields to a Sr/Rh ratio close to 10.5:7.5 per unit formula in such a way that all the oxygen polyhedra are fully occupied. Moreover, the large Sr^{2+} ions are most likely accommodated into the trigonal prismatic sites, leading to the following cationic distribution: $[Sr_{10}(Sr_{0.5}Rh_{1.5})_{TP}(Rh_6)_{Oh}]O_{24}$.

Experimental Section

The samples of the selected compositions (Sr/Rh = 12:6, 10:8 and 10:7 nominal ratios) were prepared by solid-state reaction of the appropriate stoichiometric amounts of $SrCO_3$ (Merck, 99.9%) and Rh_2O_3 (Aldrich, 99.8%). Every starting homogeneous mixture was initially heated overnight at 1000 °C, reground and then heated in air at the temperatures given in Table 3.

The cationic composition for every crystal was determined by energy dispersive spectroscopy (EDS). For this purpose, a JEOL 2000 FX electron microscope equipped with a LINK AN 10000 EDS system was employed. Thermogravimetric analysis was performed on a thermobalance based on a CAHN D-200 electrobalance, which allow the detection of variation in the oxygen content within $\pm 5 \times 10^{-3}$ on a sample of about 100 mg. The overall oxygen content was determined thermogravimetrically by reduction at 850 °C under 0.3 mbar H_2/0.2 mbar He atmosphere.

Table 3. Synthesis conditions of samples with different Sr/Rh cationic ratio.

Nominal cationic ratio Sr : Rh	T [°C]	t [h]
12:6	1050	72
	1100	48
	1150	12
10:8	1060	72
	1100	60
	1150	60
10:7	1170	72

Powder X-ray diffraction (XRD) patterns were collected at room temperature on a PHILIPS X'PERT diffractometer with a graphite monochromator and with $Cu_{K\alpha}$ radiation. The diffraction data were analysed by the Rietveld method[21] by using the Fullprof program.[22]

Selected area electron diffraction (SAED) was carried out by using a JEOL 2000 FX electron microscope fitted with a double-tilting goniometer stage (±45°). Around 50 crystals were examined in each sample in order to ascertain the homogeneity of the samples. High-resolution electron microscopy (HREM) was performed on a JEOL 4000 EX electron microscope fitted with a double-tilting goniometer stage (±25°). Simulated HREM images were calculated by the multislice method by using the MacTempas software package.

X-ray photoelectron spectroscopy (XPS) was performed in a PHI-3027 spectrometer equipped with a double pass cylindrical mirror analyser (DPCMA) by using $Mg_{K\alpha}$ radiation ($h\nu = 1253.6$ eV). XPS spectra were recorded working at a pass energy of $\Delta E = 50$ eV. Pellet samples, placed in a stainless steel holder, were introduced in the spectrometer chamber at a base pressure of 10^{-10} Torr.

Acknowledgements

Financial support of CICYT (Spain) through Research Project MAT2001–1440 (CICYT, Spain) is acknowledged. We also thank Prof. J. M. Sanz for providing XPS data and helpful discussions.

[1] J. J. Lander, *Acta Crystallogr.* **1951**, *4*, 148–156.
[2] G. Bergerhoff, O. Schmitz-Dumont, *Z. Anorg. Allg. Chem.* **1956**, *284*, 10–14.
[3] M. Evain, F. Boucher, O. Gourdon, V. Petricek, M. Dusek, P. Bezdicka, *Chem. Mater.* **1998**, *10*, 3068–76.
[4] G. R. Blake, J. Sloan, J. F. Vente, P. D. Battle, *Chem. Mater.* **1998**, *10*, 3536–47.
[5] M. Huvé, C. Renard, F. Abraham, G. Van Tendeloo, S. Amelinckx, *J. Solid State Chem.* **1998**, *135*, 1–16.
[6] M. Zakhour-Nakhl, J. B. Claridge, J. Darriet, F. Weill, H.-C. zur Loye, J. Pérez-Mato, *J. Am. Chem. Soc.* **2000**, *122*, 1618–23.
[7] K. Boulahya, M. Parras, J. M. González-Calbet, *J. Solid State Chem.* **1999**, *142*, 419–427.
[8] K. Boulahya, M. Parras, J. M. González-Calbet, *J. Solid State Chem.* **1999**, *145*, 116–127.
[9] K. Boulahya, M. Parras, J. M. González-Calbet, *Chem. Mater.* **2000**, *12*, 25–32.
[10] K. E. Stitzer, M. D. Smith, J. Darriet and H.-C. zur Loye, *Chem. Commun.* **2001**, 1680–81.
[11] K. E. Stitzer, A. El Abed, J. Darriet and H.-C. zur Loye, *J. Am. Chem. Soc.* **2001**, *123*, 8790–96.
[12] W. T. A. Harrison, S. L. Hegwood, A. J. Jacobson, *J. Chem. Soc. Chem. Commun.* **1995**, 1953.
[13] M. Hernando, K. Boulahya, A. Varela, M. Parras, J. M. González-Calbet, U. Amador, *Eur. J. Inorg. Chem.* **2002**, *4*, 805–810.

[14] A. Varela, K. Boulahya, M. Parras, J. M. González-Calbet, *Chem. Mater.* **2000**, *12*, 3237–3239.
[15] J. F. Vente, J. K. Lear, P. D. Battle, *J. Mater. Chem.* **1995**, *5*, 1785–1789.
[16] J. Campá, E. Gutierrez-Puebla, A. Monge, I. Rasines, C. Ruiz-Valero, *J. Solid State Chem.* **1994**, *108*, 230–235.
[17] M. Itoh, T. Shimura, Y. Inaguma, Y. Morij, *J. Solid State Chem.* **1995**, *118*, 206–209.
[18] S. N. Ruddlesden, S. N. Popper, *Acta Crystallogr.* **1957**, *10*, 538–539; S. N. Ruddlesden, S. N. Popper, *Acta Crystallogr.* **1958**, *11*, 54–55; S. N. Ruddlesden, S. N. Popper, *Acta Crystallogr.* **1958**, *11*, 365–368.
[19] B. L Chamberland, J. B. Anderson, *J. Solid State Chem.* **1981**, *39*, 114–117.
[20] A. L. Hector, W. Levason, M. T. Weller, *Eur. J. Solid State Inorg. Chem.* **1998**, *35*, 679–687.
[21] H. M. Rietveld, *J. Appl. Crystallogr.* **1969**, *2*, 65–71.
[22] J. Rodríguez-Carvajal, *Phys. B* **1993**, *192*, 55–69.

Received: March 28, 2002 [F3994]

  0947-6539/02/0821-4979 $ 20.00+.50/0